



## Variability Studies with SDSS

Ž. Ivezić<sup>1</sup>, R.H. Lupton<sup>1</sup>, S. Anderson<sup>2</sup> L. Eyer<sup>1</sup>, J.E. Gunn<sup>1</sup>,  
M. Juric<sup>1</sup>, G.R. Knapp<sup>1</sup>, G. Miknaitis<sup>2</sup>, J.E. Gunn<sup>1</sup>, C.M. Rockosi<sup>2</sup>,  
D. Schlegel<sup>1</sup>, M.A. Strauss<sup>1</sup>, C. Stubbs<sup>2</sup> and D.E. Vanden Berk<sup>2</sup>

<sup>1</sup>Princeton University, <sup>2</sup>University of Washington, <sup>3</sup>University of Pittsburgh

**Abstract.** The potential of the Sloan Digital Sky Survey for wide-field variability studies is illustrated using multi-epoch observations for 3,000,000 point sources observed in 700 deg<sup>2</sup> of sky, with time spans ranging from 3 hours to 3 years. These repeated observations of the same sources demonstrate that SDSS delivers  $\sim 0.02$  mag photometry with well behaved and understood errors. We show that quasars dominate optically faint ( $r \gtrsim 18$ ) point sources that are variable on time scales longer than a few months, while for shorter time scales, and at bright magnitudes, most variable sources are stars.

### 1. Introduction

The properties of optically faint variable sources are by and large unknown. There are about  $10^9$  stars brighter than  $V = 20$  in the sky, and at least 3% of them are expected to be variable at a few percent level (Eyer, 1999). However, the overwhelming majority are not recognized as variables even at the brightest magnitudes: 90% of the variable stars with  $V < 12$  remain to be discovered (Paczyński, 2000).

The Sloan Digital Sky Survey will significantly contribute to studies of optically faint variable sources due to its accurate multi-epoch photometry for a large sky area (currently 1,000 deg<sup>2</sup>, and up to 4,000 deg<sup>2</sup> by the survey completion). Here we present a preliminary variability analysis for 3,000,000 point sources detected in 700 deg<sup>2</sup> of sky, and multiply observed with time scales ranging from 3 hours to 3 years.

---

Correspondence to: [ivezic@astro.princeton.edu](mailto:ivezic@astro.princeton.edu)

### 1.1. The Basic Characteristics of the SDSS Imaging Survey

The Sloan Digital Sky Survey (SDSS; York et al. 2000; Stoughton et al. 2002) is providing homogeneous and deep ( $r < 22.5$ ) photometry in five passbands ( $u$ ,  $g$ ,  $r$ ,  $i$ , and  $z$ , Fukugita et al. 1996; Gunn et al. 1998) accurate to 0.02 mag, of up to 10,000 deg<sup>2</sup> in the Northern Galactic Cap, and a smaller, but deeper, survey of 200 deg<sup>2</sup> in the Southern Galactic Hemisphere. The survey sky coverage will result in photometric measurements for about 100 million stars and a similar number of galaxies. Astrometric positions are accurate to better than 0.1 arcsec per coordinate (rms) for sources brighter than  $20.5^m$  (Pier et al. 2003), and the morphological information from the images allows robust star-galaxy separation to  $\sim 21.5^m$  (Lupton et al. 2001).

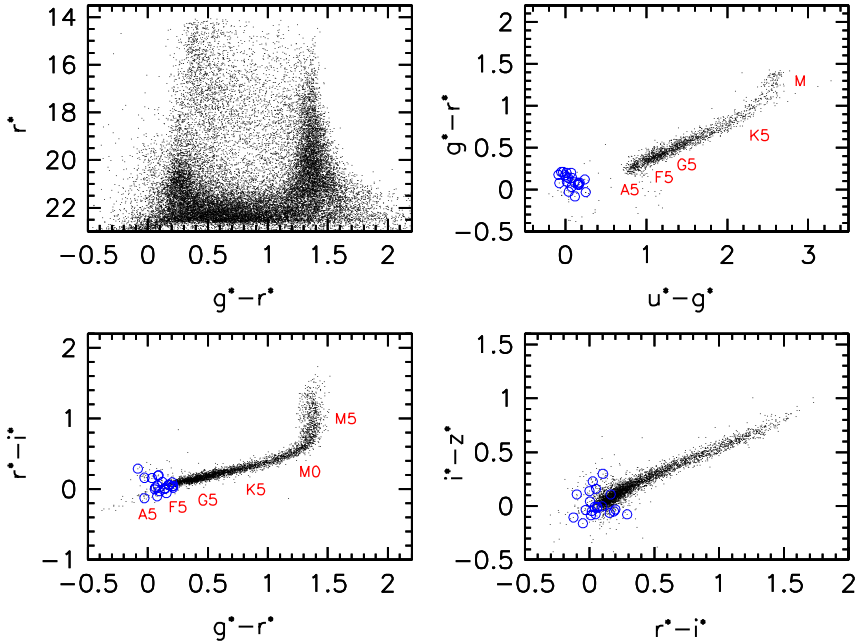


**Fig. 1.** The SDSS color-color and color-magnitude diagrams which summarize photometric properties of unresolved sources, marked as dots. The top left panel displays the  $r$  vs.  $g-r$  color-magnitude diagram for  $\sim 25,000$  objects observed in  $3 \text{ deg}^2$  of sky. The three remaining panels show color-color diagrams for objects brighter than  $20^m$  in each of the 3 bands used to construct each diagram (red is always towards the upper right corner). The locus of “normal” stars is clearly visible in all three diagrams, and the positions of several spectral types are indicated next to the locus in the  $u-g$  vs.  $g-r$  and  $r-i$  vs.  $g-r$  color-color diagrams (labels are slightly offset for clarity). Objects that have  $u-g$  and  $g-r$  colors similar to those of low-redshift ( $z < 2$ ) QSOs ( $u-g < 0.4$ ,  $-0.1 < g-r < 0.3$ ,  $r-i < 0.5$ ), and are brighter than the limit for quasars in the SDSS spectroscopic survey ( $i < 19$ ), are marked by open circles.

## 1.2. The SDSS Multi-epoch Observations

SDSS imaging data are obtained by tracking the sky in six parallel scanlines, each 13.5 arcmin wide. The six scanlines from two nights are then interleaved to make a filled stripe. Because of the scan overlaps, and because of the scan convergence near the survey poles, about 40% of the sky in the northern survey will be surveyed twice. In addition, all of the southern survey areas will be observed dozens of times to search

for variable objects and, by stacking the frames, to go deeper.

While two observations are normally insufficient to characterize a variable object, the multi-color nature and accuracy of the SDSS photometric data helps enormously. For example, the  $u$  band even allows remarkably efficient selection of the low-metallicity G and K giants (Helmi et al. 2002) and blue horizontal branch stars (Yanny et al. 2000).

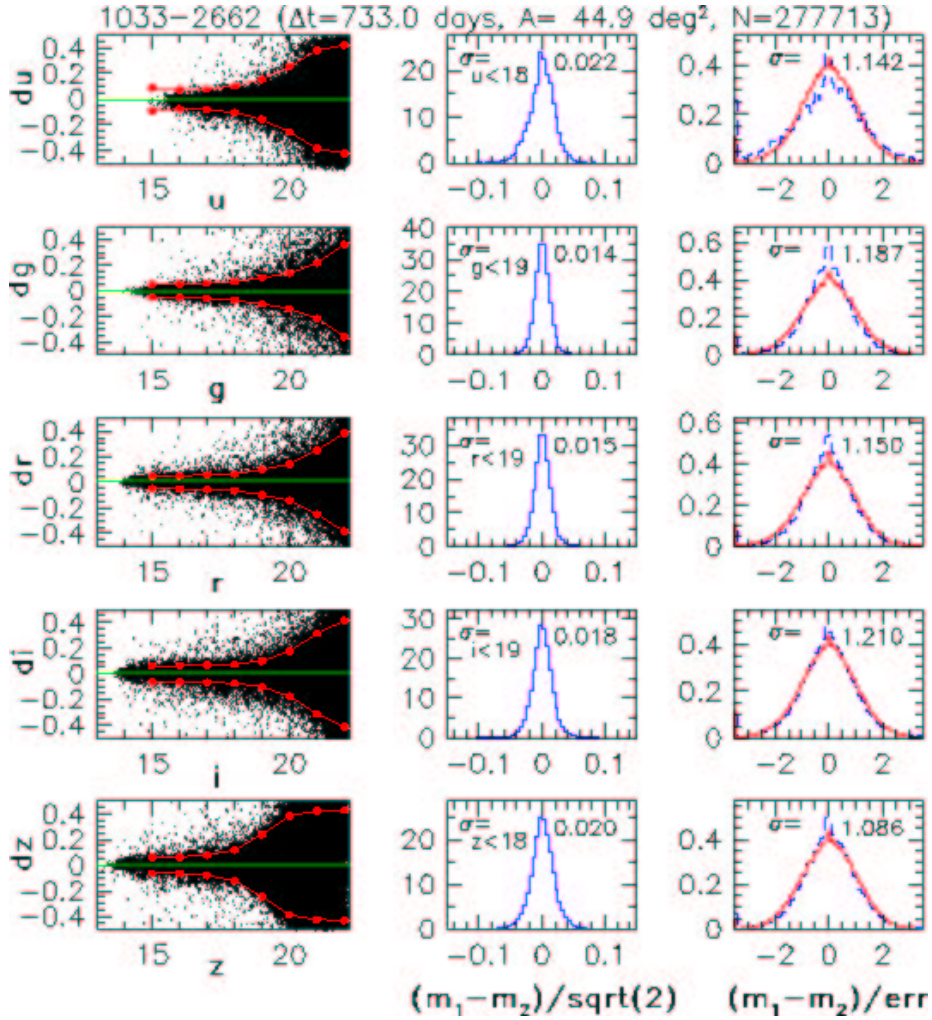


**Fig. 2.** Analysis of the SDSS photometric accuracy using repeated observations (733 days apart) of 280,000 unresolved sources detected in 45 deg<sup>2</sup> of sky. The five rows correspond to the five SDSS bands. The panels in the first column show the difference between the two measurements as a function of apparent (psf) magnitude. The big dots, connected by the lines to guide the eye, are the  $3\sigma$  envelope determined from the interquartile range in 1 mag wide bins. The middle column shows the histograms of magnitude difference divided by  $\sqrt{2}$  (a quantity representative of mean photometric errors) for the bright end, with the limiting magnitude shown in each panel. The equivalent Gaussian width of these distributions, determined from the interquartile range, is also shown in each panel. The last column displays the distribution of magnitude differences normalized by the expected formal errors. The two barely distinguishable histograms correspond to bright sources, and to the entire sample. Their mean equivalent Gaussian width,  $\sigma$ , is indicated in each panel. Note that the values of  $\sigma$  are  $\sim 1$ , testifying that the formal errors computed by the photometric pipeline are highly accurate.

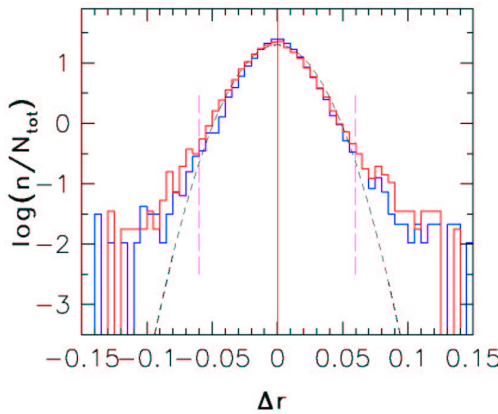


**Fig. 3.** The thick solid histograms show the distribution of the measured  $r$  band difference for two color-selected subsamples of stars observed twice 3 hours apart (note the logarithmic scale!). A Gaussian with the same interquartile range, corresponding to  $\sigma=0.02$  mag, is shown by the short-dashed line. As evident, the distribution of SDSS photometric errors is almost a perfect Gaussian.

### 1.3. The Colors of Point Sources in the SDSS Photometric System

The position of an unresolved source in multi-dimensional SDSS color space is an excellent proxy for its classification. For example, the spectral type for most stars can be estimated to within 2 spectral subtypes, or better. Furthermore, for quasars, which can be efficiently selected by their non-stellar colors (Richards et al. 2002), it is possible to obtain a reasonably accurate photometric redshift (Budavari et al. 2001, Richards et al. 2001).

The SDSS color-color and color-magnitude diagrams which summarize photometric properties of unresolved sources are shown in Figure 1. The position of a star in these diagrams is mainly determined by its spectral type. The modeling of the stellar populations observed by SDSS indicates that the vast majority of these stars (about 99%) are on the main sequence (Finlator et al. 2000).

### 1.4. How Accurate are the SDSS Data?

SDSS offers unprecedented photometric accuracy for such a large scale optical survey. Not only are the photometric errors generally small, but they themselves are accurately determined by the photometric pipeline (*photo*, Lupton et al. 2001), and can be reliably used to estimate the statistical significance of measured magnitude differences. This ability is of paramount importance for a robust statistical study of variable objects. We demonstrate these claims by comparing the measurements for  $\sim 280,000$  unresolved sources from  $45 \text{ deg}^2$  of sky observed twice 733 days apart.

The five rows of panels in Figure 2 correspond to five SDSS bands. The first column shows the difference between the two measurements as a function of apparent magnitude. At the bright end the errors are roughly independent of magnitude (because they are dominated by an imperfect description of the point-spread function), and then increase towards the faint end. As the panels in the middle column show, the internal accuracy of SDSS photometry is about 0.02 mag or better in all five bands. The SDSS is currently the only survey that provides multi-epoch imaging data to a limit as faint as  $r\sim 22$ , in an area as large as  $1000 \text{ deg}^2$ , in five bands spanning the wavelengths from UV to IR, with such small errors.

A distinctive feature of SDSS photometry is the well controlled tails of the photometric error distribution. Figure 3 shows the magnitude difference distribution for stars brighter than  $r = 19$  from  $32 \text{ deg}^2$  of sky observed twice 3 hours apart. The measured distribution closely follows a Gaussian with  $\sigma=0.02$  mag, all the way to  $\pm 3\sigma$ . There are only 0.9% observations outside the  $\pm 3\sigma$  range, in good agreement with the value expected for a perfect Gaussian (0.3%). Of course, some of these objects are certainly variable and thus increase the fraction of  $\pm 3\sigma$  outliers.

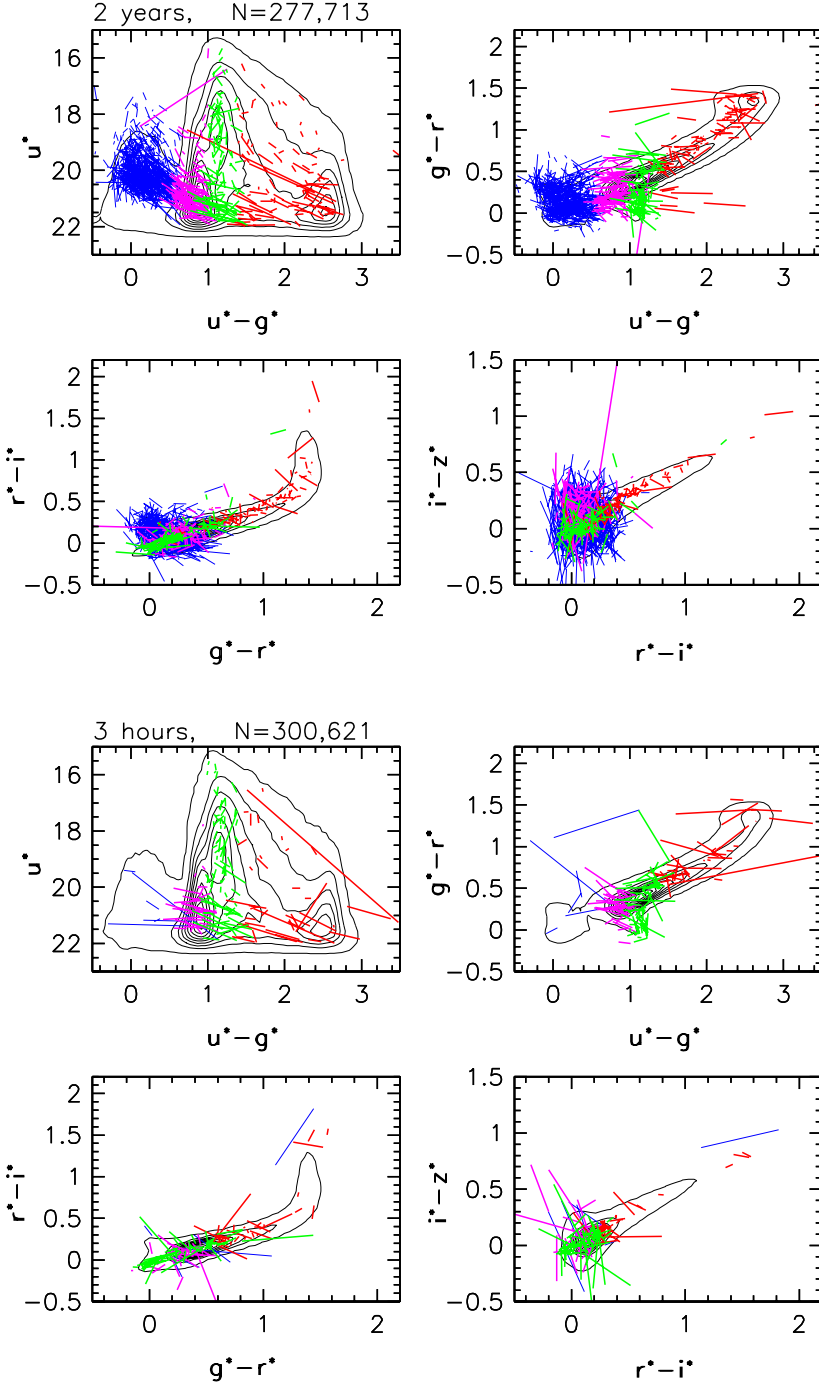


**Fig. 4.** The top four panels show variable sources discovered in  $75 \text{ deg}^2$  of sky observed twice 733 days apart. The overall source distribution is shown as contours, using the mean magnitudes. The two measurements for variable objects are connected by lines. The bottom four panels show variable sources discovered in observations obtained 3 hours apart. Note the absence of variable quasars ( $u - g < 0.6$ ) in the bottom four panels.

### 1.5. What Twinkles in the Faint Optical Sky ?

Using multiple observations of 3,000,000 point sources detected in  $700 \text{ deg}^2$  of sky, we selected variable objects by requiring a minimum variation of at least 0.075 mag in both  $g$  and  $r$  bands, and statistical significance of at least  $3\sigma$ . The variable population strongly depends on the time difference between the two observations, and also on the object's magnitude: for sufficiently long time scales (a few months or longer), variable objects fainter than  $r \sim 18$  are dominated by quasars. For time scales shorter than about a month, or at bright magnitudes, the variable objects are heavily dominated by stars.

Figure 4 shows the color-magnitude and color-color diagrams analogous to those shown in Figure 1, except that here the overall source distribution is shown as contours, using the mean magnitudes, while the two measurements for variable objects are connected by lines. The top four panels correspond to observations obtained 733 days apart, and the bottom four panels to observations obtained 3 hours apart. A good handle on the types of detected variable sources can be obtained by simply studying their  $u-g$  color distribution. For a  $\sim 2$  year time scale, the majority of objects (77%) have colors typical of low-redshift quasars ( $u-g < 0.6$ ). Blue stars consistent with the halo turn off, both in colors and in apparent magnitude, make up 40% of the remaining objects (this subsample may also contain some quasars), and the reddish stars with  $u-g > 1.3$  another 40%. RR Lyrae stars, which can be easily recognized thanks to their distinctive colors (Ivezić et al. 2000), comprise 20% of detected variable stars. At the 3 hours time scale, only about 2% of variable objects have quasar colors. RR Lyrae now make up 35% of the sample, mainly because the number of red stars is much smaller (the surface density of selected RR Lyrae is about 1 per  $\text{deg}^2$ , nearly independent of time scale and galactic coordinates). The smaller number of red

stars is consistent with them being long-period (Mira) variables which don't appreciably vary on time scales of several hours.

For a more detailed description of this work please see Ivezić et al. and Vanden Berk et al. (in prep.).

**Acknowledgements.** Funding for the creation and distribution of the SDSS Archive has been provided by the Alfred P. Sloan Foundation, the Participating Institutions, the National Aeronautics and Space Administration, the National Science Foundation, the U.S. Department of Energy, the Japanese Monbukagakusho, and the Max Planck Society. The SDSS Web site is <http://www.sdss.org/>.

The SDSS is managed by the Astrophysical Research Consortium (ARC) for the Participating Institutions. The Participating Institutions are The University of Chicago, Fermilab, the Institute for Advanced Study, the Japan Participation Group, The Johns Hopkins University, Los Alamos National Laboratory, the Max-Planck-Institute for Astronomy (MPIA), the Max-Planck-Institute for Astrophysics (MPA), New Mexico State University, University of Pittsburgh, Princeton University, the United States Naval Observatory, and the University of Washington.

## References

- Budavári, T., et al. 2001, AJ, 122, 1163
- Eyer, L. 1999, Baltic Astronomy, 8, 321
- Finlator, K., et al. 2000, AJ, 120, 2615
- Fukugita, M., Ichikawa, T., Gunn, J.E., et al. 1996, AJ, 111, 1748
- Gunn, J.E., et al. 1998, AJ, 116, 3040
- Helmi, A., et al. 2002, ApJ, in press; also astro-ph/0211562
- Ivezić, Ž., et al. 2000, AJ, 120, 963
- Lupton, R.H. et al. 2001, astro-ph/0101420
- Paczyński, B. 2000, PASP, 112, 1281
- Pier, J., et al. 2003, AJ, in press (March 2003)
- Richards, G., et al. 2001, AJ, 122, 1151
- Richards, G., et al. 2002, AJ, 123, 2945
- Yanny, B., et al. 2000, ApJ, 540, 825.
- York, D.G., et al. 2000, AJ, 120, 1579